Physics of Rotating Space Elevators

Leonardo Golubović* and Steven Knudsen

Physics and Astronomy Department, West Virginia University,

Morgantown, WV 26506-6315, USA

*E-mail: lgolubov@wvu.edu

Abstract: The physics of Space Elevators connecting the Earth with outer space has recently attracted increased attention, in part due to the discovery of ultra-strong materials such as carbon nanotubes and diamond nano-thread structures. In this article we review a new venue in space elevator physics: Rotating Space Elevators (RSE) [L. Golubović and S. Knudsen: "Classical and statistical mechanics of celestial scale spinning strings: Rotating space elevators", Europhysics Letters 86(3), 34001 (2009)]. The RSE is a double rotating system of strings reaching outer space. Objects sliding along the RSE string (sliding climbers) do *not* require internal engines or propulsion to be transported far away from the Earth's surface. The RSE thus solves a major problem in the space elevator technology which is how to supply the energy to the climbers moving along the string. RSE strings exhibit interesting nonlinear dynamics and statistical physics phenomena. Satellites and spacecraft carried by sliding climbers can be released (launched) along RSEs. RSE strings can host space stations and research posts. Sliding climbers can be then used to transport useful loads and humans from the Earth to these outer space locations.

Keywords: *Space Elevator, Inertial Forces, Classical Mechanics, Statistical Physics, Space Travel, Nonlinear Dynamics, Instabilities and Transitions, Chaos*

1. Introduction

The physics of Space Elevators connecting the Earth with outer space has attracted increased attention in this millennium [1]. This interest emerged in part due to the discovery of ultra-strong materials such as carbon nanotubes [2,3] and diamond nano-thread structures [4]. Space elevators are celestial scale examples of physical systems with reduced dimensionality such as the strings, polymers, and membranes [5,6,7].

Recently, we introduced a new concept in this physics area: Rotating Space Elevator (RSE) [8-11]. In this review article we discuss this new venue in space elevator physics. The RSE is a double rotating floppy string reaching extraterrestrial locations. Interestingly, objects sliding along the RSE string (climbers) do not require internal engines or propulsion to be transported far away from the Earth's surface. The RSE thus solves a major problem in space elevator physics which is how to supply energy to the climbers moving along space elevator strings.

2. Historic background: The conceptual development of the traditional Space Elevator

Dreams of traveling to the heavens have entranced men since the early times of civilization. The story of the "Tower of Babel" in Genesis 11 of the Bible connects the notion of human cooperation for space travel to "heaven" to the multiplying of human languages, which frustrates the effort. In modern history, the fable "Jack and the Beanstalk," from 1807 (and a burlesque version named *The Story of Jack Spriggins and the Enchanted Bean* from 1734) presents a young boy whose mother plants foolishly obtained seeds which then grow into a great tower that can even hold a giant! Neither of these stories addresses the physics questions of how the towers can remain upright under compressive and buckling (bending) forces.

It was therefore up to the famous Russian scientist Konstantin Tsiolkovsky in 1895 to integrate the vision of the space elevator with the realities of physics [1]. Tsiolkovsky was considered to be a rocket scientist and the father of spaceflight and he had spent considerable time thinking about the limitations and alternatives of rocket flight. He was inspired by the Eiffel Tower in Paris to conceptualize a tower that reached from ground zero all the way into deep space, above the geosynchronous satellite orbit. This "celestial castle" would orbit the Earth in a geosynchronous fashion meaning that it would be directly overhead one spot on Earth's surface at all times. An object released at the tower's top would also have the orbital velocity necessary to remain in geosynchronous orbit. Thus, the

Tsiolkovsky's tower can be used to deploy satellites into orbits around the Earth.

The centrifugal force due to Earth rotation acting on celestial towers has an interesting effect: A tall enough tower is under *tension* rather than compression, and therefore is not subject to the sorts of buckling that limits the height of skyscrapers. In the case of skyscrapers, the centrifugal force is negligible, but for the celestial size objects envisioned by Tsiolkovsky and his followers, both scientists and science fiction writers such as Arthur C. Clarke [12,13] the gravitational force and centrifugal force play equally significant roles. Because the internal force is a tension rather than compression, the space elevator can be a floppy non-rigid object ("string").

It wasn't until 1960 that someone suggested a feasible method for building the space elevator. Another Russian scientist, Yuri N. Artsutanov, conceived a scheme for building a space tower [14,15]. Artsutanov proposed using a geosynchronous satellite as the starting point from which to construct the tower. By using a counterweight, a cable would be lowered from the satellite down to the Earth surface while the counterweight was extended from the satellite away from Earth, keeping the center of gravity of the cable motionless relative to the rotating Earth. This construction scheme is still the standard [1].

Jerome Pearson [16] brought the idea of the space elevator to the scientific community in the U.S. In his careful and detailed design of a workable space elevator while at the U.S. Air Force Flight Dynamics Laboratory he outlined, mathematically and physically, the implications of a space elevator string designed to obey the constraint of constant stress (tension/cross sectional area) throughout, while maintaining an external force balance. Artsutanov independently proposed the same idea [14,15]. The two balancing external forces in the earth frame are the centrifugal and gravitational forces. The Pearson-Artsutanov constant stress elevator provides a simple way to handle the high tensions present in space elevators: The elevator can be designed for *any* given value of the constant stress. This value is can be chosen to be smaller than the critical breaking stress of the material used. Hence, from the materials science point of view, real space elevators *can* be made. This spurred a lot of recent interest in building space elevators out of novel materials such as carbon nanotubes [1-3].

It is very easy to understand the advantages of the space elevator concept over conventional rocket propulsion. With chemical propulsion, a rocket carries its own fuel that it needs to overcome gravitational forces, leading to intrinsic energy inefficiency. Because of earth's deep gravitational well, the load-to-fuel ratios are typically very small (e.g., ~ 10^{-2} for the Apollo/Saturn V missions to the Moon), so that essentially all fuel energy is used to accelerate the fuel itself. On the other side, within the space elevator concept, a spaceship climbs along the elevator via an internal electrical engine which uses externally supplied electric energy. Since there is no fuel carried by the climber, the supplied energy is 100% used to lift the climber. So, the space elevator concept is immensely more energy efficient than the rocket propulsion.

The problem however remains on how to externally supply the energy to the climber. Naively, one may think of running an electrical transmission line along the space elevator, until realizing just how long this structure is compared to transmission lines on earth, so that power losses will be close to 100%. To remedy this, Edwards proposes that laser power be beamed up the elevator from the ground to the climber [1]. The beam energy would be absorbed by climbers and converted into electrical energy driving their engines. For any of these schemes climbing is typically slow and it may take several months for the climber to travel along the space elevator from the Earth to the geosynchronous level. During such a long climb, the useful load (including possibly humans) would be exposed for a very long time to dangerous cosmic radiation, which is especially strong in this range of altitudes above the Earth. Even without this problem with cosmic rays, typically long travel time itself is certainly not a satisfactory feature of space elevators, especially if a rapid deployment of objects into outer space is desired.

These were the motivations for us to introduce a completely novel space elevator concept described in the following.

3. Rotating Space Elevator (RSE): Solution of the climber energy supply problem

In this review article we discuss a new class of nonlinear dynamical systems, Rotating Space Elevators (RSE). The RSE concept has been introduced for the first time by us in [8] and elaborated in detail in our subsequent studies [9-11].

The RSEs are multiply rotating systems of strings. Remarkably, useful loads and humans *sliding* along the RSE strings do *not* require internal engines or propulsion to be rapidly transported (sled) into space far away from the Earth's surface; see section 4 discussions. Thus, the RSE concept solves the major problem of energy supply to climbers that troubles the ordinary LSE concept.

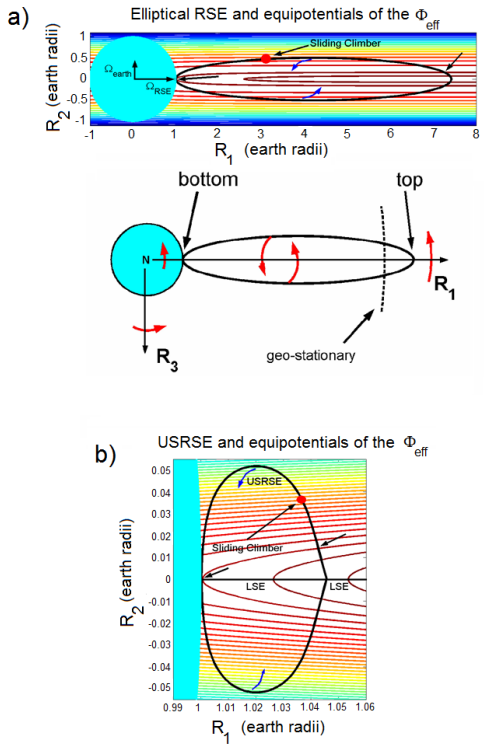

Figure 1 - In (a) upper panel, the elliptical RSE with minor semi-axis b= 0.5 Earth radii and major semi-axis a = 3.2107 Earth radii (so its top is about 0.8 Earth radii above the geo-stationary level). In (a) lower panel, a different view on the RSE. The coordinate system (R_1, R_2, R_3) rotates together with the Earth around the R_2-axis pointing through the north pole N. Indicated are the internal (nearly around the R_1-axis) and geo-synchronous (together with the Earth) rotations of the RSE. The RSE is tied to the Earth at its bottom point. In (b), we show the USRSE (attached to a LSE) with T_{RSE} = 4.22 min (discussed in sect. 4). In these figures we also include the equipotentials of the effective potential in eq. (7). Sliding climbers oscillate between two turning points (indicated by straight arrows) that are on the same equipotential. Adapted from [9].

The RSE is a *double* rotating floppy string typically having the shape of a loop as in Figure 1. Due to its special kind of motion (see below), the RSE becomes pre-tensioned due to gravitational and inertial forces. Due to the tension, the floppy RSE maintains its loopy shape.

The special RSE motion, ensuring the persistence of its shape, is a nearly a geometrical superposition of: (a) geosynchronous (one-day period) rotation around the Earth, i.e. the R_2-axis in Figure 1, and (b) yet another rotational motion of the string which is typically much faster (with period ~ tens of minutes) and goes on around a line perpendicular to the Earth at its equator (the R_1 axis in Figure 1).

This second, *internal rotation* plays a very special role: It provides the dynamical stability of the RSE shape and, importantly, it also provides a mechanism for the climbing of objects free to slide along the RSE string.

RSE can be used to elevate climbers from the surface of the Earth to remote outer space locations in a simple way; see Sec. 4. Remarkably, the climbers in Figure 1 do not need any internal engine to execute their motion. Rather, they *spontaneously* slide along the RSE string from the Earth to outer space locations. This unusual climber sliding motion is facilitated by the inertial force (centrifugal force) acting on climbers due to the RSE's internal rotation. In section 6 we describe possible use of RSE to launch satellites and interplanetary spaceships.

The RSE can be made in various shapes. The simple double rotating geometrical motion can be made to represent an approximate yet exceedingly accurate solution to the exact equations of the RSE string dynamics. This RSE feature is accomplished by a special ('magical') choice of mass distribution of the RSE cable; see Sec. 4. This RSE feature is corroborated by numerical simulations showing that (under the conditions discussed in Sec. 5) the RSE double rotation motion as well as nearly constant RSE shape can both persist indefinitely in time [8,9,10].

The elliptical RSE in Figure 1(a) exhibits very high tensile stresses at its points near mid-height. Therefore, other shapes were described whose mass distribution yields a Uniform Stress RSE (USRSE) [8,9]. The USRSE, displayed in Figure 1(b), can be made by using technologically available materials such as carbon nanotubes; see section 4.

4. The physics of RSE

In this section we review the basic physics of RSE [8]. For simplicity, let us consider inextensible limit in which the RSE floppy string obeys the Newtonian equation of motion

$$\mu(s)\frac{\partial^2 \vec{R}}{\partial t^2} = \frac{\partial}{\partial s} T(s,t) \frac{\partial}{\partial s} \vec{R} + \vec{f}_{ext} . \qquad (1)$$

In Eq. (1), $\vec{R}(s,t)$ are 3-D space positions of string points parametrized by their arc-length distances s [thus, $|\partial \vec{R}(s,t)/\partial s| = 1$]. $\mu(s)$ in Equation (1) is the string's local mass line density, while $T(s,t)$ is the local value of the string's tension field, and

$$\vec{f}_{ext}$$

are external forces (per unit length) acting on the string. Prominent among them is the force of the Earth gravity, for which,

$$\vec{f}_{ext}^{\,grav} = \mu(s)\ \vec{a}_{grav} ,$$

with

$$\vec{a}_{grav} = -\frac{\partial \Phi_{grav}}{\partial \vec{R}}.$$

Here,

$$\Phi_{grav}(\vec{R}) = -\frac{GM_{earth}}{|\vec{R}|},$$

is the Earth's gravitational potential with M_{earth} = the Earth's mass. $T(s,t)$ is obtained by solving Eq. (1) combined with the local constraint $|\hat{t}(s,t)| = 1$, with $\hat{t}(s,t) = \partial \vec{R}/\partial s$. In the presence of a sliding climber of mass m_{cl} at the arc-length distance $s(t)$, i.e., at the 3-D position $\vec{R}^{cl}(t) = \vec{R}(s(t),t)$, the external force density acting on the RSE, $\vec{f}_{ext}$ in Eq. (1) includes also the term

$$\vec{f}_{ext}^{\,cl} = -\delta(s - s(t))\ \vec{N},$$

where $\vec{N}$ is the normal force exerted by the climber on the string; $\vec{N} \cdot \hat{t} = 0$. The climber dynamics is governed by the second Newton's law,

$$m_{cl} \frac{d^2 \vec{R}^{cl}}{dt^2} = \vec{N} + \vec{F}_{ext},$$

with $\vec{F}_{ext}$ signifying (other than $\vec{N}$) external forces acting on the climber, e.g., the Earth's gravity,

$$\vec{F}_{ext}^{\,grav} = m_{cl}\ \vec{a}_{grav} = -m_{cl} \frac{\partial \Phi_{grav}}{\partial \vec{R}}.$$

Using the constraint $|\hat{t}(s,t)| = 1$, from the above equation,

$$\ddot{s}(t) = \hat{t} \cdot \left(\frac{\vec{F}_{ext}}{m_{cl}} - \frac{\partial^2 \vec{R}}{\partial t^2} \right), \qquad (1')$$

and

$$\vec{N} = -(\vec{F}_{ext})_{\perp} + m_{cl} \left(\frac{\partial^2 \vec{R}}{\partial t^2} \right)_{\perp} + m_{cl} \frac{\partial \hat{t}}{\partial s} [\dot{s}(t)]^2 + 2 m_{cl} \frac{\partial \hat{t}}{\partial t} \dot{s}(t)$$

with:

$(\vec{V})_{\perp} = \vec{V} - \hat{t}(\hat{t} \cdot \vec{V})$ for any vector $\vec{V}$.

Space elevators such as RSE are most naturally discussed by using *non-inertial reference frames*. In a non-inertial frame rotating with the angular velocity $\vec{\Omega}$, inertial forces have to be included into $\vec{f}_{ext}$ and $\vec{F}_{ext}$ in Eqs. (1) and (1'), yielding

$$\vec{f}_{ext} = \mu(s)\ (\vec{a}_{grav} + \vec{a}_{inert}),$$
$$\vec{F}_{ext} = m_{cl}\ (\vec{a}_{grav} + \vec{a}_{inert}), \qquad (2)$$

with,

$$\vec{a}_{inert} = \vec{\Omega} \times (\vec{R} \times \vec{\Omega}) + \vec{R} \times \frac{d\vec{\Omega}}{dt} + \frac{d\vec{R}}{dt} \times 2\vec{\Omega};$$

see [17]. In the geosynchronous frame (used in the simulations and the figures displayed here) rotating with the period = $2\pi/\Omega_{earth}$ = one day, Eq. (3) is employed with

$$\vec{\Omega} = \vec{\Omega}_{earth} = \hat{e}_2 \Omega_{earth},$$

with unit vector $\hat{e}_2$ along the Earth polar axis and the equator in the *(R_1, R_3)* plane; see Figs. 1(a) and (b). In the simulations, at $t = 0$ the RSE is initially in the *(R_1, R_2)* plane. To initiate the double rotation motion, the RSE is given initial spin around the R_1-axis, with the angular velocity Ω_{RSE}. The RSE bottom point is tied to the Earth to provide access for the sliding climbers starting there their trip into outer space; see also Sec. 7. Other than this, *the RSE moves purely under the influence of inertia and gravity.*

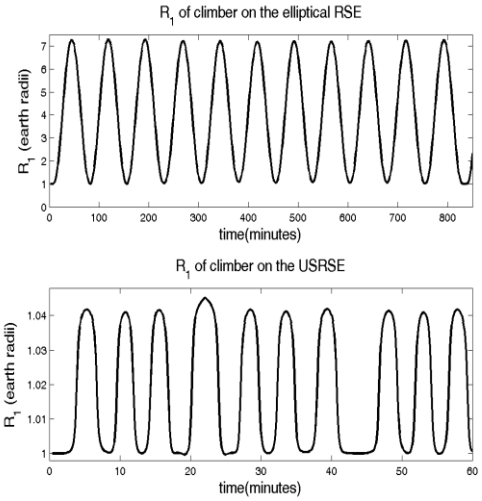

Figure 2 - From the simulations of Ref. 9: The upper panel: The $R_1(t)$ coordinate of the climber which slides with no friction along the floppy RSE with the (initial) shape in Figure 1(a) and T_{RSE}=10.83 min. The lower panel: The $R_1(t)$ coordinate of the climber on the floppy RSE with initial shape in Figure 1(b) with T_{RSE}=4.22 min. See Sec. 4 for the analytic explanation of the nearly periodic character of climber motion. Note: With a weak sliding friction, climbers would eventually stop near the RSE point minimizing the $U(s) = \Phi_{eff}(\vec{R}(s))$. From the equipotentials of the effective potential labeled in Figure 1, one can see that this point occurs close to the RSE point maximizing its R_2 coordinate in Figure 1.

A remarkable effect of the RSE double rotation motion is that it facilitates a physical mechanism which efficiently moves sliding *engine free* climbers from the surface of the Earth to remote extraterrestrial locations. As evidenced by the simulations in Figure 2, a sliding climber starting at rest close to the Earth *spontaneously* oscillates between its initial position and a turning point in outer space. The nearly

periodic character of the climber's motion is explained later on in this section.

Another remarkable effect is an enduring stability of the RSE sizes and orientation and the persistence the RSE's double rotation motion which is provided by a specially chosen form of the mass line density $\mu(s)$; see Eq. (8) below and Figure 3. This effect is documented by the simulations results displayed in Figure 4 [8,9].

These two outstanding RSE effects are revealed by considering the system in the (natural for the RSE) *double rotating frame* (DRF) obtained from the geosynchronous (single rotating) frame by adding to it the rotation around the R_1-axis in Figs. 1(a) and (b). The net angular velocity of the DRF is thus

$$\vec{\Omega}(t) = \vec{\Omega}_{RSE} + \vec{\Omega}_{earth}(t).$$

Here,

$$\vec{\Omega}_{RSE} = \Omega_{RSE}\hat{e}_1$$

corresponds to the rotation around the R_1-axis while

$$\vec{\Omega}_{earth}(t)$$

is the Earth's angular velocity vector which in the DRF rotates with the angular velocity $-\Omega_{RSE}$ (and thus acquires a time-dependence). With the above $\vec{\Omega}(t)$, in DRF the Eq. (3) yields

$$\vec{a}_{inert} = -\frac{\partial \Phi_{inert}}{\partial \vec{R}} + \vec{a}_{res}, \tag{4}$$

with

$$\Phi_{inert}(\vec{R}) = -\frac{1}{2}\Omega_{earth}^2 R_1^2 - \frac{1}{2}(\Omega_{RSE}^2 + \frac{1}{2}\Omega_{earth}^2)(R_2^2 + R_3^2) \tag{5}$$

being a *time-independent* effective potential generating inertial forces sensed in the DRF. The residual, $\vec{a}_{res}$ term in Eq. (4) includes velocity dependent terms that vanish for an object *at rest in the DRF,* as well as *fast time-dependent* oscillatory terms of $\vec{a}_{inert}$ (with frequencies Ω_{RSE} and $2\Omega_{RSE}$ >> Ω_{earth}) that have *zero* time average over one RSE period ($T_{RSE} = 2\pi/\Omega_{RSE}$); see [9]. For the here interesting situations with $T_{RSE}=2\pi/\Omega_{RSE}$ ~ 10min << $T_{earth}=2\pi/\Omega_{earth}$=1 day, one has $\Omega_{RSE} >> \Omega_{earth}$ and the potential term in Eq. (4) dominates over the $\vec{a}_{res}$ term [8,9]. Thus, Eq. (2) reduces to

$$\vec{f}_{ext} \cong -\mu(s)\ \frac{\partial \Phi_{eff}}{\partial \vec{R}},$$
$$\vec{F}_{ext} \cong -m_{cl}\ \frac{\partial \Phi_{eff}}{\partial \vec{R}} \tag{6}$$

with the net effective potential,

$$\Phi_{eff}(\vec{R}) = \Phi_{grav}(\vec{R}) + \Phi_{inert}(\vec{R}) = -G\frac{M_{earth}}{|\vec{R}|} + \Phi_{inert}(\vec{R}). \tag{7}$$

The time *independence* of this effective potential allowed us in [8] to find a special ('magical') mass distribution $\mu(s)$ with which the RSE string *indefinitely* maintains its initial shape by remaining at rest in the DRF. For a given flat RSE string shape specified by a 2-d curve

$$\vec{R}(s) = [R_1(s), R_2(s), R_3(s) = 0]$$

this special mass line density $\mu(s)$ is obtained from Eq. (1) with $\partial^2\vec{R}/\partial t^2 = 0$ and $\vec{f}_{ext}$ as in Eq. (6). The resulting differential equations for $T(s)$ and $\mu(s)$ can be integrated exactly, yielding the magical mass line density $\mu(s)$ [8,9],

$$\ln\left[\frac{\mu(s)}{\mu(0)}\right] = -\int_0^s ds'\ \frac{(\vec{a}_{net}(s')\cdot\hat{t}(s'))}{K(s')} + \ln\left[\frac{K(s=0)}{K(s)}\right] \tag{8}$$

where

$$\vec{a}_{net} = -\frac{\partial \Phi_{eff}}{\partial \vec{R}},$$

is evaluated at the RSE point [$R_1(s)$,$R_2(s)$], whereas

$$K(s) = -\frac{(\vec{a}_{net}(s)\cdot\hat{n}(s))}{C(s)} = \frac{T(s)}{\mu(s)}. \tag{8'}$$

In Eq. (8'), $C(s)$ is the local RSE string curvature; $C(s) = d\theta/ds$ with $\theta(s)$ the angle between the tangent unit vector $\hat{t}(s) = \partial\vec{R}/\partial s$ and the R_1-axis in Figs. 1(a) and (b). The unit vector $\hat{n}(s)$ makes the angle $\theta(s)+\pi/2$ with the R_1-axis.

The magical mass distributions obtained by applying Eq. (8) to the (initial) RSE shapes in Figure 1, which are used in the simulations discussed in this paper, are shown in Fig. 3. Our simulations [8-10], which are free of the approximation Eq. (6) employed in Eq. (8), indeed show (under the conditions discussed in Sec. 5 in the following) a remarkable stability of the RSE sizes and orientation provided by the magical mass distribution in Eq. (8). We note that $\mu(s) = \rho\ A(s)$, with ρ the density of the RSE material and $A(s)$=the string cross-sectional area (which can vary along the RSE by tapered cable design). Thus, by Eq. (8'), the tensile stress obeys the relation,

$$p(s) = \frac{T(s)}{A(s)} = \rho\ K(s)\,. \qquad (8'')$$

The RSE displayed in Figure 1(b) is a *uniform stress* RSE (USRSE) for which the tensile stress $p(s)$ is s-independent. For an USRSE, by Eq. (8''), the $K(s) = K = const.$ With this condition, Eq. (8') yields the second order differential equation

$$\frac{d^2R_2}{dR_1^{\,2}} = -\frac{1}{K}\left[1+\left(\frac{dR_2}{dR_1}\right)^2\right]\left[a_2 - a_1\frac{dR_2}{dR_1}\right], \qquad (8''')$$

with $a_i = -\partial\Phi_{eff}\,/\,\partial R_i\,;\ i = 1,\ 2$. Differential equation Eq. (8''') can be used to obtain a USRSE shape for *any* given K and T_{RSE}. Figure 1(b) shows thus obtained USRSE shape for T_{RSE}=4.22min and $K = \tilde{K}\ v_1^{\,2}$. Here, $v_1=(GM_{earth}/R_{earth})^{1/2}$=1st cosmic speed=7.89km/sec [R_{earth}=the Earth radius], whereas $\tilde{K}$ is a dimensionless constant.

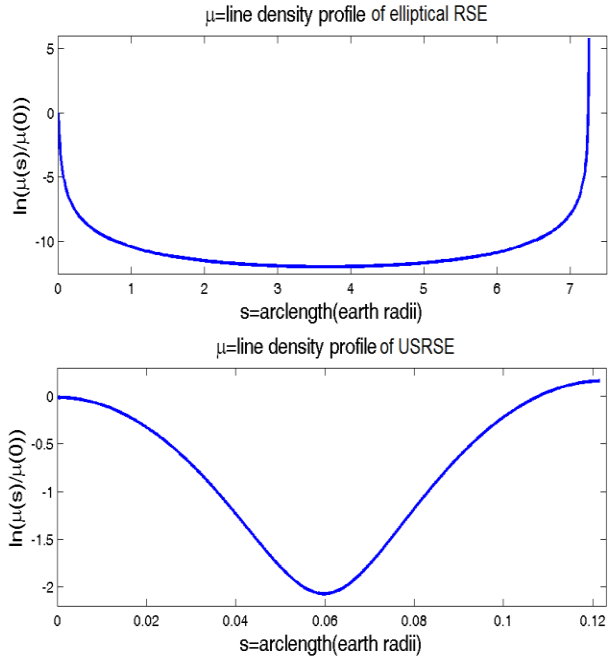

Figure 3 - The upper panel: the magical mass distribution [i.e., line density obtained by Eq. (8)] of the RSE with the shape in Figure 1(a) and T_{RSE} =10.83 min. The lower panel: the magical mass distribution (line density) of the RSE with the shape in Figure 1(b) and T_{RSE} =4.22 min. Adapted from [9].

For the USRSE in Figure 1(b), we set $\tilde{K} = 1/4$, corresponding, by Eq. (8''), to the USRSE tensile stress $p = \tilde{K}\rho\ v_1^{\,2} = 20.24\ GPa$ if the USRSE is made of carbon nano-tubes (CNT) with $\rho \approx 1{,}300 kg/m^3$. Thus, pleasingly, the tensile stress p of this USRSE is smaller than the tensile strengths $p_{\max} \approx 60\ GPa$ of single-wall CNT, and $p_{\max} \approx 150\ GPa$ of multi-wall CNT [2,3]. *So, this* USRSE *is technologically achievable with modern day materials.* By Eq. (8) with $K(s) = K = const.$, and by

$$-\vec{a}_{net}\cdot\hat{t} = (\partial\Phi_{eff}\,/\,\partial\vec{R})\cdot(\partial\vec{R}\,/\,\partial s) = \partial\Phi_{eff}(\vec{R}(s))\,/\,\partial s$$

we find that the USRSE magical mass line density obeys the equation

$$\ln\left[\frac{\mu(s)}{\mu(s_1)}\right] = \ln\left[\frac{A(s)}{A(s_1)}\right] = \frac{\Phi_{eff}(\vec{R}(s)) - \Phi_{eff}(\vec{R}(s_1))}{K} \qquad (8'''')$$

for any *(s,s₁)*. It is depicted in lower panel of Figure 3 for the USRSE in Figure 1(b) [with T_{RSE}=4.22 min, and $\tilde{K} = 1/4$], with $s_1 = 0$ corresponding to the USRSE bottom at the Earth. This line density profile can be technologically achieved by using tapered cable having the cross-sectional area *A(s)* given by our Eq. (8''''). The USRSE in Figure 1(b) is attached to a Linear Space Elevator (LSE) which can also be designed to have a uniform stress $< p_{\max}$ [16]. The LSE line mass density has a discontinuity at the junction between the USRSE and the LSE (to balance the USRSE tension force pulling down the LSE along the R_1-axis). Away from the junction, the uniform stress LSE line mass density obeys Eq. (8'''') with $\vec{R}(s)$= *(R_1=s, R_2=0, R_3=0)*, [16]. We note that unlike the technologically achievable USRSE in Figure 1(b) with $p < p_{\max}$ (for CNT), the Earth based elliptic RSE in Figure 1(a) has a *non*-uniform stress that exceeds the CNT tensile strength in the midsection of the RSE. However, elliptic RSEs built on dwarf planets such as asteroids Ceres and Vesta would have a tensile stress $p < p_{\max}$ (for CNT). They are thus technologically achievable.

Periodic like motion of sliding climbers (seen in the simulations in Figure 2) goes on along nearly constant shape RSE strings. This climber motion can be understood by means of Eq. (6). For a time-independent RSE shape $\vec{R}(s)$, the Eq. (1'), in combination with Eq. (6), reduces to

$$\ddot{s} = -\hat{t}(s)\cdot\frac{\partial\Phi_{eff}}{\partial\vec{R}(s)} = -\frac{\partial\vec{R}(s)}{\partial s}\cdot\frac{\partial\Phi_{eff}}{\partial\vec{R}(s)} = -\frac{\partial\Phi_{eff}(\vec{R}(s))}{\partial s}$$

yielding the conservation law

$$\frac{1}{2}\left(\frac{ds(t)}{dt}\right)^2 + \Phi_{eff}[\vec{R}(s(t))] = const. \qquad (9)$$

Eq. (9) is isomorphic to the familiar conservation law describing oscillatory 1-d motion of a particle with the position $s(t)$ in the potential

$$U(s) = \Phi_{eff}(\vec{R}(s)) .$$

Strikingly, in this potential, sliding climbers simply oscillate between two turning points, one of which is close to the Earth (starting point) whereas the other one is in outer space; see Figs. 1 and 2. In fact, the RSE bottom (the point $s = 0$) becomes a local maximum of the potential $U(s)$ (seen by sliding climbers) provided the RSE angular frequency Ω_{RSE} is bigger than the minimal frequency [8,9],

$$\Omega_{\min} \cong \frac{v_1}{R_{earth}}(1 + R_{earth} \mid C(s=0) \mid)^{1/2}$$
$$= \frac{v_1}{R_{earth}}(1 + \frac{1}{\tilde{K}(s=0)})^{1/2} \qquad (10)$$

with $\tilde{K}(s) = K(s)/v_1^2$ [8,9]. Due to this, $\Omega_{RSE} > \Omega_{\min}$, i.e., $T_{RSE} < T_{\max} = 2\pi/\Omega_{\min}$, a climber initially at rest will start moving up no matter how close is its initial position to the RSE bottom $[R_1 = R_{earth}, R_2 = R_3 = 0)]$ in Figs. 1(a) and (b), at $s = 0$. For the elliptical RSE in Figure 1(a) with the semi-axes b=0.5R_{earth}, a=3.2107R_{earth}, the climbing threshold RSE period $T_{\max} = 22.71\text{min}$. This is bigger than the T_{RSE} of 10.83min of the elliptic RSE in Figure 1(a), yielding the oscillatory sliding climber dynamics seen in the simulations in Figure 2, upper panel. For an USRSE with $\tilde{K}(s) = 1/4$, by Eq. (10), $T_{\max}$=37.78min. This is bigger than the T_{RSE} of 4.22min of the USRSE in Figure 1(b), yielding the oscillatory sliding climber dynamics seen in the simulations in Figure 2, lower panel. We note that the USRSE point having the maximum distance R_2 away from the R_1 – axis in Figure 1(b) has the speed $\Omega_{RSE} \cdot (R_2)_{\max} \cong v_1$ =1st cosmic speed (for the USRSE with T_{RSE}=4.22 min). Thus, the USRSE loop in Figure 1(b) can be used for launching satellites. We will discuss potential applications of the RSE in Sec. 6. It is significant to note that [by using differential Eq. (8''')] the USRSE loops can be designed with their bottoms anywhere above the Earth surface (e.g., above the dense atmospheric layer, to avoid air-resistance).

5. Shape stability of RSE and crumpling transition

Numerical simulations of RSEs reveal an interesting morphological phase transition of the RSE strings that occurs with changing the (initial) RSE angular frequency Ω_{RSE}, i.e., its period T_{RSE} [8-10].

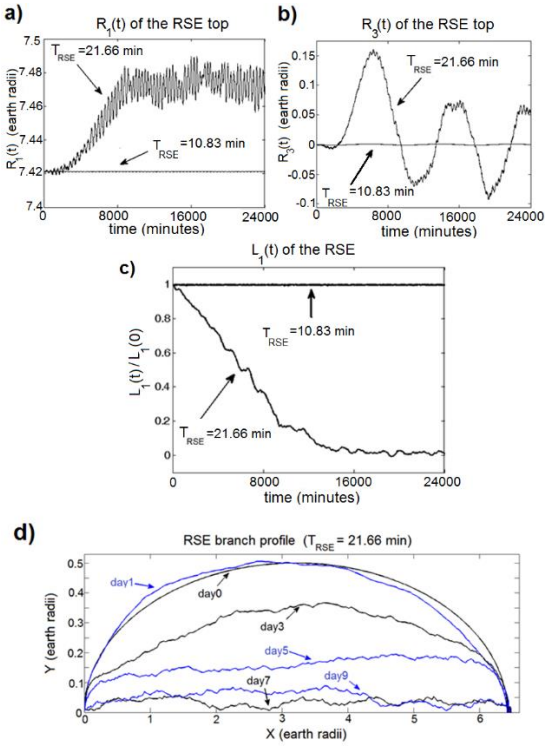

Figure 4 - From the simulations in [9]: For the elliptic RSE in Figure 1(a), the RSE top coordinates R_1(t) in (a), R_3(t) in (b), and, in (c), the evolution of the RSE angular momentum L_1 about the R_1-axis (in the frame rotating with the Earth), for T_{RSE} =10.83min and T_{RSE} =21.66min. In (d), the evolution of the RSE profile (of one of its two branches), for T_{RSE} =21.66min over the first ten days. Here, for any RSE point P, the Y is its distance away from the (instantaneous) axis A connecting the RSE bottom and top, and the X is the distance between the normal projection of P onto the axis A and the RSE bottom point (at X=0).

This transition was seen both in the USRSE and the elliptical RSE. E.g., for the elliptical RSE in Fig 1(a), it occurs at a critical value for the RSE period $T_{crit} \approx 17\text{ min}$. For $T_{RSE} < T_{crit}$, the tension field $T(s,t)$ remains everywhere positive. It exhibits only small oscillations around $T(s, t=0) > 0$ given by Eqs. (8) and (8'). However, for $T_{RSE} > T_{crit}$, the RSE string (in both the elliptical

RSE and the USRSE) undergoes a dramatic shape change and chaotic long-time dynamics: Tension field develops a noise like behavior in which $T(s,t)$ assumes both positive and negative values. In effect, the RSE string *crumples* due

to the buckling of the string sections that are under locally negative $T(s,t)$.

Macroscopically, the string crumpling triggers a narrowing of the RSE initial shape, displayed in Figure 4(d) for the elliptical RSE with T_{RSE} =21.66min. The narrowing eventually turns initially elliptic RSE into two nearly independently fluctuating linear type space elevators connecting the massive elevator top and bottom regions. Chaotic dynamics of the two elevator's branches reflects an ergodic-like (thermal equilibrium like) string state similar to that of the directed polymers [5] stretched between the RSE top and bottom.

Related to the RSE narrowing is the dynamics of the RSE angular momentum L_1 about the R_1-axis (in the frame rotating with the Earth as in Figure 1); see Figure 4(c) for the elliptical RSE with T_{RSE}=21.66min: The L_1 decays to zero over a two-week period. [In contrast to this, for $T_{RSE}>T_{crit}$, the USRSE narrows and loses its L_1 only partially.] As seen in Figs 4(a) and (b) at T_{RSE}=21.66min, these phenomena destabilize the position of the elliptical RSE top. It drifts away from its initial position (at 0.8 Earth radii above geostationary level) to a new slightly higher position around which the RSE top continues to chaotically oscillate.

In drastic contrast to this, for $T_{RSE} < T_{crit}$, the string shapes of both the elliptic RSE and the USRSE remain nearly the same as in their initial configuration in Figs. 1(a) and (b), i.e., no RSE narrowing occurs. Related to this, as evidenced in Figure 4(c) for the elliptical RSE with T_{RSE} =10.83min, the RSE angular momentum L_1 is nearly constant in time, whereas the RSE top exhibits only very small oscillations around its initial position; see Figure 4(a) and (b).

6. Using RSEs to launch spaceships and satellites

By the discussions of Sec. 4, RSE is a rapid extraterrestrial transportation system which requires no internal engines for the climbers sliding along the elevator strings. Climbers motion is naturally facilitated by employing basic natural phenomena, the inertial forces due to the internal RSE rotation around the R_1-axis in Figure 1. As noted before in Sec. 4, RSEs can be used to launch satellites and interplanetary spaceships [8,9]. In this section we will discuss this RSE capability in more detail. It is also significant to note that the RSE strings can be used to host space stations and research posts. Sliding climbers can be then used to transfer useful loads and humans from the Earth to these extraterrestrial locations. Satellites and spaceships transported by sliding climbers can be released (launched) along RSEs. Let us look at a climber that has started its motion at near rest at the RSE tying position with the Earth in Figure 1 [there, $|\vec{R}(s=0)| = R_{earth}$]. Let us then look at an object released from the climber when it reaches the RSE position

$$\vec{R}(s) = [R_1(s), R_2(s), R_3(s) = 0]$$

in the DRF. The released object's speed in the DRF, that is its speed along the tangent at $\vec{R}(s)$ is *ds/dt*. This tangential velocity is obtained by Eq. (9) yielding,

$$\frac{1}{2}\left(\frac{ds(t)}{dt}\right)^2 = \Phi_{eff}[\vec{R}(s(0)=0)] - \Phi_{eff}[\vec{R}(s(t))] \tag{11}$$

Using here the Eqs. (5) and (7), we find,

$$\frac{1}{2}\left(\frac{ds(t)}{dt}\right)^2 = -G\frac{M_{earth}}{R_{earth}} + G\frac{M_{earth}}{|\vec{R}(s)|} + \frac{1}{2}\Omega_{earth}^2[R_1(s)]^2 + \frac{1}{2}(\Omega_{RSE}^2 + \frac{1}{2}\Omega_{earth}^2)[R_2(s)]^2 \tag{12}$$

Of the practical interest is the released object speed observed in the *inertial frame.* Consider, for example, the situation in which the object is released when the elevator, 9 is in the plane of Figure 1(a, upper panel) or Figure1 (b) (then the R_2 axis of DRF points along the north-south direction). Let the object be released from a climber which is on the *lower branch* of RSE in Figure 1. The RSE velocity at this point is in the direction of the Earth rotation and has the magnitude

$$v_{RSE} = \Omega_{RSE}|R_2(s)| + \Omega_{earth}R_1(s), \tag{13}$$

in the inertial frame. This velocity points into the plane of Figure 1. In addition to this velocity, the released object also has the tangential velocity *ds/dt* which is in the plane of Figure 1. Thus, by Pythagorean Theorem, the total released object speed in the inertial frame, $v_{released}$ satisfies

$$v_{released} = \sqrt{(v_{RSE})^2 + (ds/dt)^2}. \tag{14}$$

By Eqs. (12) through (14), the speed of the released object in the inertial frame satisfies the equation

$$\frac{1}{2}(v_{released})^2 = -G\frac{M_{earth}}{R_{earth}} + G\frac{M_{earth}}{|\vec{R}(s)|} + (\Omega_{RSE}^2 + \frac{1}{4}\Omega_{earth}^2)[R_2(s)]^2 + \Omega_{RSE}\Omega_{earth}|R_2(s)|R_1(s) + \Omega_{earth}^2[R_1(s)]^2, \tag{15}$$

if the object is released when the elevator loop is in the plane of Figure 1(a, upper panel) or Figure 1 (b), from a climber which is on the lower branch of RSE in Figure 1. If

this speed is large enough, the released object will unbind from the Earth, and approach infinity with the speed V_∞ ("escaping speed") that can be obtained from the mechanical energy conservation law,

$$\frac{1}{2}(v_\infty)^2 = \frac{1}{2}(v_{released})^2 - G\frac{M_{earth}}{|\vec{R}(s)|}. \qquad (16)$$

By Eqs. (15) and (16),

$$\frac{1}{2}(v_\infty)^2 = -(v_1)^2 + [\Omega_{RSE}R_2(s)]^2\left[1+\left(\frac{\Omega_{earth}}{2\Omega_{RSE}}\right)^2 + \frac{\Omega_{earth}R_1(s)}{\Omega_{RSE}R_2(s)} + \left(\frac{\Omega_{earth}R_1(s)}{\Omega_{RSE}R_2(s)}\right)^2\right]. \qquad (17)$$

Above, we introduced the first cosmic speed

$$v_1 = (GM_{earth}/R_{earth})^{1/2} = 7.89 km/\sec.$$

Again, we stress that the Eq. (17) applies if the object is released when the elevator loop is in the plane of our Figure 1(a, upper panel) of Figure 1(b), from a climber which is on the lower branch of RSE in Figure 1. This particular case is significant because the enhancement of the released object speed provided by the rotation of the Earth is at its maximum (for the RSE rotating around the R_1 axis in the direction indicated in Figure 1). For the interesting (for RSE systems) situations with $\Omega_{RSE}>>\Omega_{earth}$ [see the discussions following Eq. (5)], the results in Eqs. (13), (15) and (17) reduce to approximate yet more illuminating results,

$$v_{RSE} \approx \Omega_{RSE}\,|R_2(s)|, \qquad (13')$$

$$\frac{1}{2}(v_{released})^2 \approx -G\frac{M_{earth}}{R_{earth}} + G\frac{M_{earth}}{|\vec{R}(s)|} + \Omega_{RSE}^2[R_2(s)]^2, \qquad (15')$$

while the escaping speed ("speed at infinity") approximately satisfies the simple equation,

$$\frac{1}{2}(v_\infty)^2 \approx -(v_1)^2 + [\Omega_{RSE}R_2(s)]^2. \qquad (17')$$

The approximate results (13'), (15'), and (17') are equivalent to ignoring the Earth rotation (setting Ω_{earth}=0) in the exact results in Eqs. (13), (15), and (17). Thus, the above approximate results are significant also because they (approximately) apply to the objects released from the RSE at any orientation of the rotating RSE plane relative the R_1-R_2 plane in Figure 1. [We stress that $|R_2(s)|$ in the above equations is the distance between the release point and the R_1 axis.]

The approximate results (13'), (15'), and (17') offer a better insight into the launching actions of the RSE. By Eq. (17'), the released object (spaceship) will escape to an interplanetary travel [$(v_\infty)^2 > 0$] if the RSE speed of the release point of ($=\Omega_{RSE}|R_2(s)|$) is bigger than the first cosmic speed v_1. By the Eq. (17'), the highest possible escaping speed V_∞ is achieved if the object is released from a sliding climber at the RSE point with the maximum value of $|R_2|$. For example, for the elliptic RSE in the figure 1(a), this point is the midpoint of the RSE, with $|R_2|_{max}=b=0.5R_{earth}$ at $R_1=a+R_{earth}=4.2107\ R_{earth}$. At this point, with $T_{RSE}=10.83$ *min*, one has $\Omega_{RSE}|R_2(s)|=3.9v_1$. With this value, the Eq. (17') predicts the value of the highest possible escaping speed (speed at infinity) from this RSE to be $(v_\infty)_{\max} \approx 5.3310 v_1$ which is only slightly smaller than $v_\infty = 5.5200 v_1$ as obtained by using the exact Eq. (17). We note that for the marginal case with $\Omega_{RSE}|R_2(s)|=v_1$, whence the approximation Eq. (17') predicts $v_\infty = 0$, the exact equation (17) yields an $(v_\infty)^2 > 0$, meaning that the object still unbinds with a small escape velocity at infinity. A situation like this is (incidentally) realized in the USRSE in the Figure 1(b), with T_{RSE}=4.22 min. For its point with the maximum value of $|R_2|$ ($|R_2|_{max}=0.052R_{earth}$ at $R_1=1.02R_{earth}$) we find $\Omega_{RSE}|R_2(s)|=1.04v_1$ (which is only slightly above v_1). The approximate Eq. (17') would then yield $v_\infty \approx 0.4040 v_1$, whereas the exact Eq. (17) gives $v_\infty = 0.54303 v_1$ for this case [if the object is released when the elevator loop is in the plane of our Figure 1, from a climber which is on the lower branch of USRSE in Figure 1(b)].

The shape of a USRSE loop is determined by solving the differential equation (8'''), and thus it depends on the value of $T_{RSE}=2\pi/\Omega_{RSE}$. In Figure 5 (upper panel), we display the USRSE shapes for several different values of T_{RSE}, all for the same value of the parameter $\tilde{K} = 1/4$ (corresponding to the string tensile stress $p = 20.24 GPa$ if the USRSE is made of carbon nano-tubes, see Sec. 4). In Figure 5 (lower panel), we plot, versus T_{RSE}, the USRSE speed $\Omega_{RSE}|R_2(s)|_{\max}$ as well as the speed at infinity V_∞ of an object released from a climber at $|R_2(s)|_{\max}$ on the lower branch of USRSE in Figure 1(b) when this branch is in the plane of our Figure 1. With a known RSE shape, this speed can be calculated from Eq. (17). Note that V_∞ vanishes at a characteristic value of T_{RSE} of about 6 min.

Thus far we have discussed the case with no sliding friction between the climber and the RSE string. Only then Eq. (9) applies. The friction may be significantly depressed, e.g., by magnetic levitation. With some friction present, climbers would eventually stop near the RSE point minimizing the effective potential seen by the climber in DRF,

$$U(s) = \Phi_{eff}(\vec{R}(s)).$$

From the equipotentials displayed in Figure 1, this point occurs very close to the RSE point maximizing its R_2 coordinate in Figure 1. Interestingly, as noted above, the USRSE point having the maximum distance $|R_2|$ away from the R_1-axis in Figure 1(b) has the speed $\Omega_{RSE} \cdot |R_2|_{\max} \cong v_1$ = 1st cosmic speed (for the particular USRSE shown in Figure 1(b), with T_{RSE}=4.22 min and $\tilde{K} = 1/4$; see Sec. 4) Thus, the USRSE loop in Figure 1(b) can be used for launching satellites carried from the Earth by a sliding climber. Indeed, due to the friction, the climber would eventually stop close to the USRSE point having the maximum distance away from the R_1 – axis in Figure 1(b). At this point, the stopped climber rotates with the RSE with the speed $\cong v_1$=1st cosmic speed. Thus, the climber can directly release the carried satellite into a nearly circular low Earth orbit.

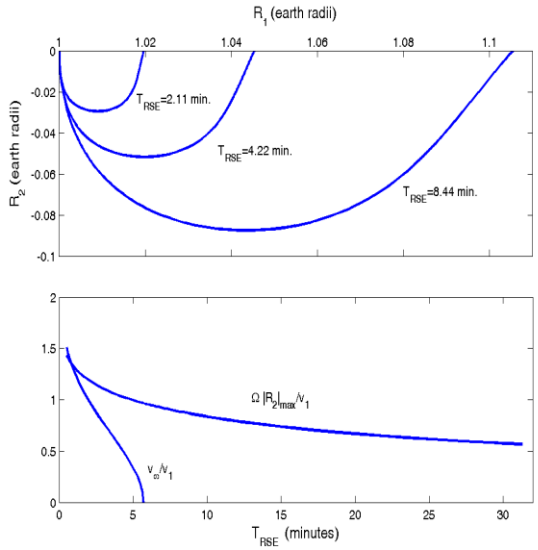

Figure 5 - In the upper panel, we plot the USRSE loop shapes obtained for several different values of T_{RSE}, all for the same value of the parameter $\tilde{K} = 1/4$. In the lower panel, we plot, versus T_{RSE}, the USRSE speed $\Omega_{RSE}|R_2(s)|_{\max}$ as well as the speed at infinity v_∞ of an object released from a sliding climber at $|R_2(s)|_{\max}$ on the lower branch of USRSE in Figure 1(b) when this branch is in the plane of our Figure 1. It is obtained from Eq. (17). The two speeds are given in units of the first cosmic speed v_1. Adapted from [9].

7. Physics of Untied RSE and Celestial Dumbbells

In this review article we also discuss basic physics of *celestial scale dumbbells* such as the Analemma Tower suspended from an asteroid orbiting the Earth [18]. Celestial dumbbells involve two large masses (top and bottom) connected by strings. The two masses move geosynchronously with the Earth, with the bottom mass remaining close to the Earth and the top mass moving above the Earth's geosynchronous satellite orbit. Notable and unusual examples of celestial scale dumbbells are untied Rotating Space Elevators (RSE) [10]. Elliptic RSE is similar to celestial dumbbells such as the Analemma Tower because it has a large mass concentration in the top and bottom regions of the loop; see figure 3, upper panel.

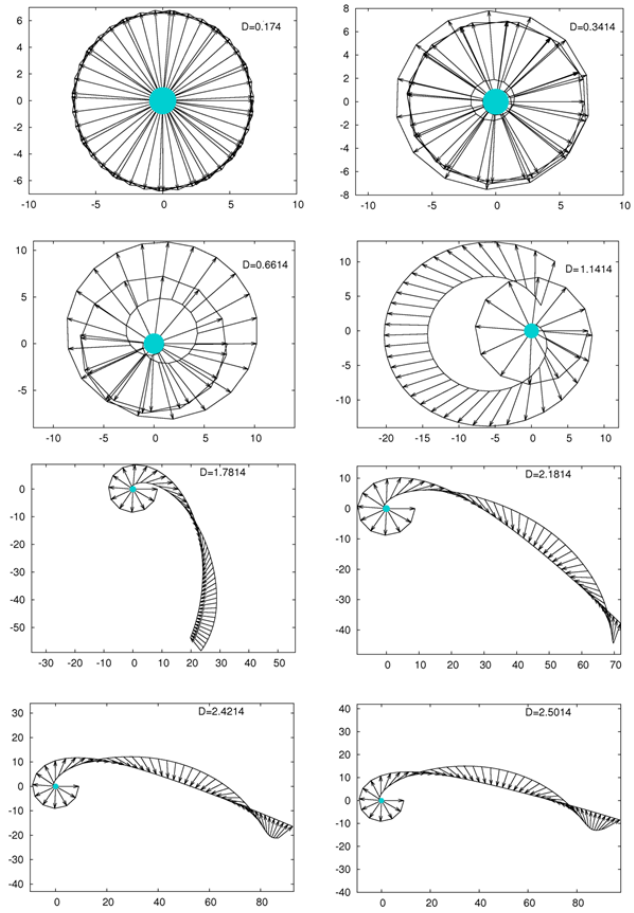

Figure 6 - From simulations of *floppy* untied RSE; adapted from [10]. The RSE is conceptualized as an arrow with head being the RSE top and end of tail being the RSE bottom. The Earth is depicted as a small circle. The length unit used here is 1 Earth radius. Each panel gives a time sequence of RSE bottom and top projections onto the equatorial plane in the *inertial frame*, over the first 6000 min of time evolution.

What will happen if one *unties* the bottom of the elliptic RSE (ERSE) in Figure 1 from the Earth? This interesting question is investigated by us in [10]. Interestingly, it was found that the tying of the bottom may not be needed at all to achieve the stable double rotating motion of ERSE. In fact, the magical mass distribution $\mu(s)$ in Eq. (8) does *not*

assume that the loopy ERSE is tied to the Earth. Thus, it is in principle possible that an untied ERSE exhibits persistent shape and everlasting double rotating motion much like the tied ERSE. This intriguing possibility was explored by studying the dynamics of the untied elliptical RSE [10]. The actual untied ERSE behavior was found to crucially depend on the distance *D* ("gap") between the ERSE top and the geostationary satellite orbit (with the radius of 6.6108 Earth radii). Celestial dumbbells exhibit interesting nonlinear dynamics [10]. Thus, the untied RSE loop may still behave as if it were tied to the planet. Such a quasi-tied yet untied RSE loop remains close to the Earth and exhibits persistent shape and enduring double rotating motion. Moreover, the climbers sliding along such a quasi-tied RSE move in much the same way as they do along a tied RSE.

Under some conditions however geosynchronous orbits of untied celestial scale dumbbells, such as untied RSE and Analemma Tower, may undergo an instability leading them to a dynamical state in which the dumbbell hops well above the Earth surface; see figure 6. This hopping regime occurs if the dumbbell top initial height above geostationary orbit *D* is bigger than $D_{hopping} \cong 0.2$Earth radii. By increasing the gap *D* above the hopping threshold $D_{hopping}$, the maximum height reached during hopping increases and eventually *diverges* at the characteristic gap value $D_{unbinding} \cong 2.1$ Earth radii. Such a celestial scale dumbbell *unbinds* from the Earth and escapes to infinity, i.e., to interplanetary space.

8. Summary

In summary, the RSEs are rapid outer space transportation systems that require no internal engines for the climbers sliding along the elevator strings. RSE strings exhibit interesting nonlinear dynamics and statistical physics phenomena. RSEs' action fundamentally employs truly basic natural phenomena -- gravitation and inertial forces. Satellites and space-crafts carried by sliding climbers can be released (launched) along RSEs. RSE strings can host space stations and research posts. Sliding climbers can be then used to transport useful loads and humans from the Earth to these outer space locations. The RSE exhibits a variety of interesting dynamical phenomena explored by numerical simulations. Thanks to its special design aided by its magical mass distribution, the RSE exhibits persistent shape and enduring double rotating motion. Under some conditions however the RSE may undergo a morphological transition to a chaotic state reminiscent of fluctuating directed polymers encountered in the statistical physics of strings and membranes.

Acknowledgments

We thank WVHTC and NASA for the sub-grant WVHTC-W-NASA-IR-07-1367 of the Grant NNX06AE557: Innovative Research for Next Generation Space Exploration.

References

[1] B. C. Edwards and E. A. Westling: "*The Space Elevator: A RevolutionaryEarth-to-Space Transportation System"* (BC Edwards, USA, 2003).

[2] T. C. Fitzgibbons, et al. "*Benzene-derived carbon Nanothreads"*, Nature Materials **14**, 43-47 (2014).

[3] M. F. Yu et al.: "*Tensile Loading of Ropes of Single Wall Carbon Nanotubes and their Mechanical Properties*", Physical Review Letters **84**, 5552-5555 (2000).

[4] M. F. Yu et al.: "*Strength and breaking mechanism of multiwalled carbon nanotubes under tensile load",* Science **287**, 637-640 (2000).

[5] M. Kardar: "*Statistical Physics of Fields"* (Cambridge University Press, 2007).

[6] D. R. Nelson: "*Defects and Geometry in Condensed Matter Physics"* (Cambridge University Press, Cambridge, 2002).

[7] D. R. Nelson, T. Piran, and S. Weinberg, S. (Eds.): *"Statistical Mechanics of Membranes and Surfaces"* (World Scientific, Singapore, 1988).

[8] L. Golubović and S. Knudsen: "*Classical and statistical mechanics of celestial scale spinning strings: Rotating space elevators",* Europhysics Letters **86**(3), 34001 (2009).

[9] S. Knudsen and L. Golubović: "*Rotating space elevators: Physics of celestial scale spinning strings*", European Physical Journal Plus **129**, 242 (2014).

[10] S. Knudsen and L. Golubović: "*Physics of untied rotating space elevators",* European Physical Journal Plus **130**, 243 (2015).

[11] S. Knudsen and L. Golubović: *"Modeling the physics of sliding objects for Rotating Space Elevators",* European Physical Journal Plus **131**, 400 (2016).

[12] A. C. Clarke: "*The Fountains of Paradise"* (Harcourt Brace Jovanovich, New York, 1978).

[13] A. C. Clarke: "*The Space Elevator: 'Thought Experiment' or Key to the Universe?",* Advances in Earth Oriented Applied Space Technology Vol. 1, 39-48 (1981). Retrieved from:

http://www.islandone.org/LEOBiblio/CLARK1.HTM

[14] Y. V. Artsutanov: "*V Kosmos na Elektrovoze" ("To the Cosmos by Electric Train"),* Komsomolskaya Pravda (in Russian), front page of Sunday Supplement (July 31, 1960). English translation retrieved from:

http://www.spaceward.org/documents/Artsutanov_Pravda_SE.pdf

[15] V. Lvov: "*Sky-Hook: old idea",* Science **158,** 946-947 (1967).

[16] J. Pearson*: "The Orbital Tower: A Spacecraft Launcher Using the Earth's Rotational Energy". Acta Astronautica **2**, 785–799 (1975).*

[17] L. D. Landau and E. M. Lifshitz: "*Mechanics*, *Course in Theoretical Physics, Vol. 1"* (Pergamon Press, London, 1976).

[18] Clouds AO: "*Analemma Tower"* (2017). Retrieved from http://www.cloudsao.com/ANALEMMA-TOWER